Electronic Supplementary Material (ESI) for Journal of Materials Chemistry A.

$FeSe_2$ micro-nanorods confined in N-doped carbon as an advanced anode for fast sodium ion storage

Shilin Zhou,[a] Rui Jiang,[a] Shige Wang,[a] Lu Yu,[a] Xiaoyan Shi,[a] Lianyi Shao,[a] Zhipeng Sun*[a] and Lifeng Hang*[b]*

[a] School of Materials and Energy, Guangdong University of Technology, Guangzhou 510006, Guangdong, China. E-mail: shaolianyi@gdut.edu.cn, zpsunxj@gdut.edu.cn.

[b] Department of Medical Imaging, Guangdong Second Provincial General Hospital, Guangzhou, 518037, Guangdong, China. E-mail: hanglf@ustc.edu.cn

Materials characterization

The compositions were confirmed by X-ray diffraction (XRD, Rigaku SmartLab). The structure and morphology of all products were studied by scanning electron microscope (SEM, Phenom Workstation) and transmission electron microscope (TEM, Thermo FEI: Talos F200S). X-ray photoelectron spectroscopy (XPS, K-Alpha) was used to assess the chemical makeup of the samples. To confirm the carbon content, thermal gravimetric analysis (TGA) was implemented by the SLTG-1 Thermal Analyzer instrument. Tap density was tested by LABULK0335.

Electrochemical measurements

The electrode slurry was produced by mixing active materials ($FeSe_2$@NC), conductive materials (super P), and binder (sodium carboxymethyl cellulose) with a weight ratio of 7:2:1 in water and then stirring several times. The slurry was ultimately coated on Cu foil and dried at 80 ℃ for one night and the mass of the active materials was controlled about 1.0~1.5 mg cm^{-2}. Na foil, glass fiber (GF/D), and 1.0 M $NaPF_6$ in diglyme were applied as counter/reference electrode, separator, and electrolyte to make a half-cell in an argon-filled glove box. The charge/discharge tests were performed on NewareBST76 in 0.01-3.0 V. Cyclic voltammetry (CV) curves and electrochemical impedance spectroscopy (EIS) were obtained on the electrochemical workstation (CHI760).

NVPF@rGO, a conductive material (Super P), and the adhesive (polyvinylidene fluoride) with a mass ratio of 8:1:1 were mixed in appropriate N-methyl-2-pyrrolidinone to obtain the slurry. The slurry was evenly coated on the aluminum foil, dried at 80 °C for 12 h, and then cut into discs with a diameter of 12 mm to form the positive electrode. For the full battery, the $FeSe_2$@NC/Na battery was discharged/charged at 0.1 A g^{-1} for 2 cycles to activate the electrode. Then full battery consisting of NVPF@rGO cathode and $FeSe_2$@NC-450℃-1h anode was assembled in an argon-filled glovebox using 1 M $NaPF_6$ in diglyme as the electrolyte.

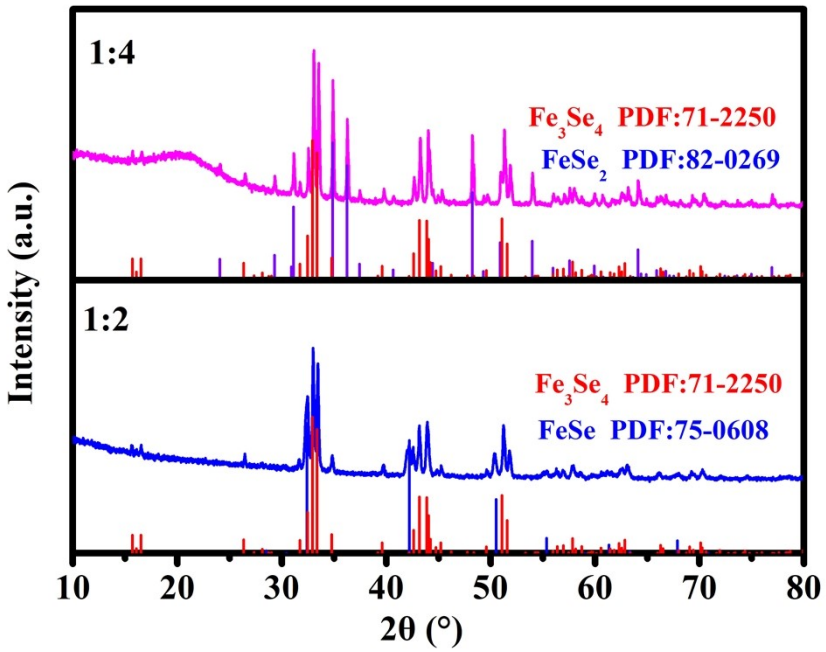

Fig. S1 XRD patterns of samples prepared by sintering FeOOH and selenium powder at the ratios of 1:4 and 1:2.

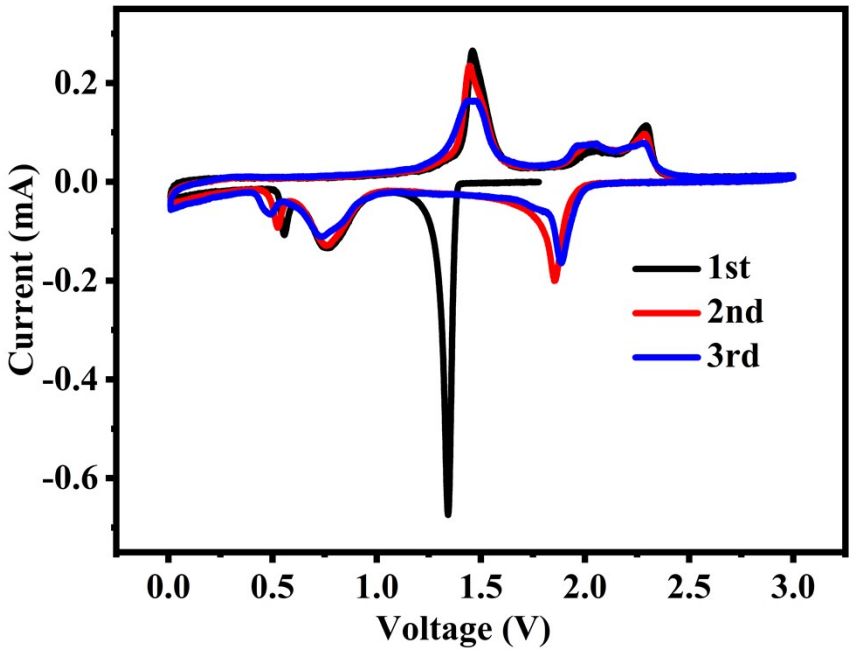

Fig. S2 CV curves of $FeSe_2$@NC in the first three cycles.

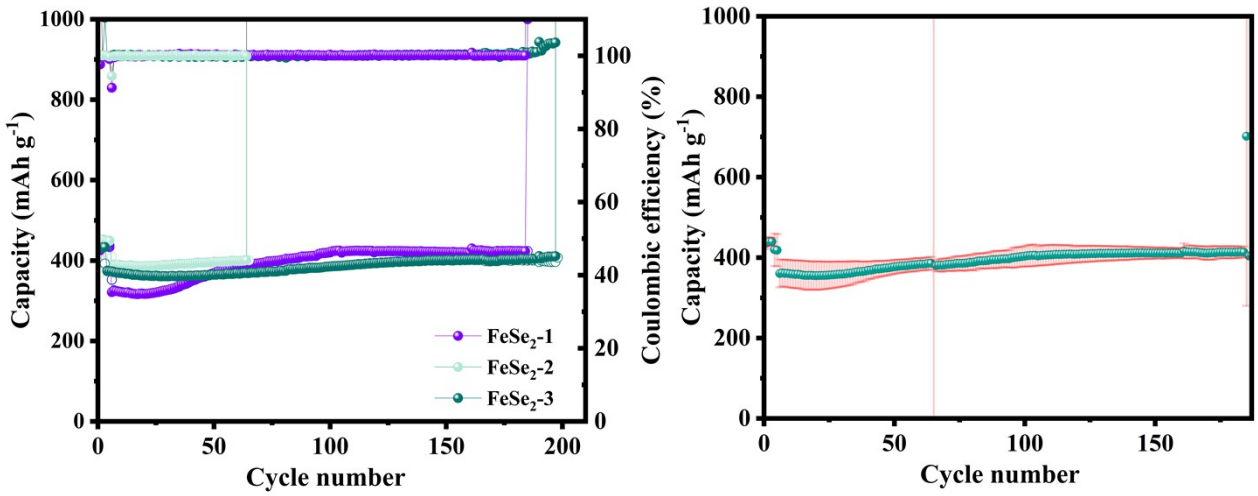

Fig. S3 (a) Electrochemical performance and (b) error bars of $FeSe_2$.

In order to avoid the chance of the experiment, the cycle performance of three half cells for $FeSe_2$ were supplied with error bars in Fig. S3. The standard deviation of the three data is between 5 and 30. The standard deviation is too large when the battery dies.

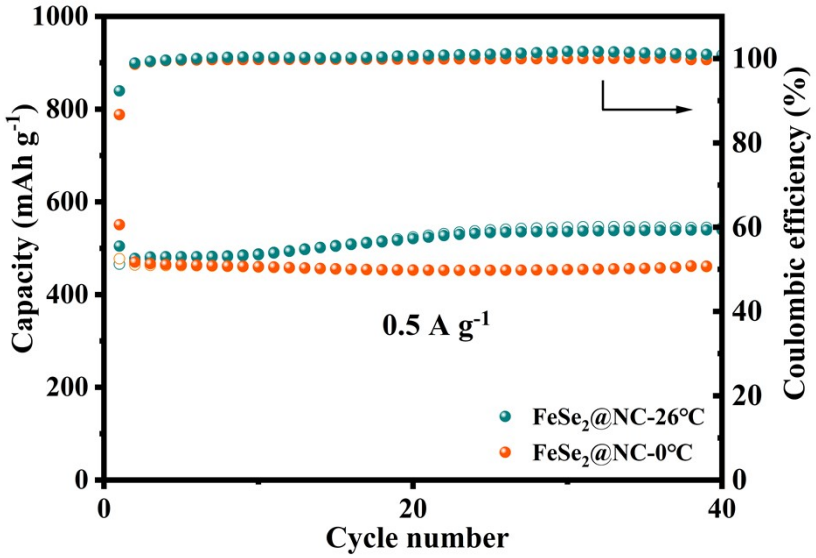

Fig. S4 Electrochemical performance of $FeSe_2$@NC at different temperatures.

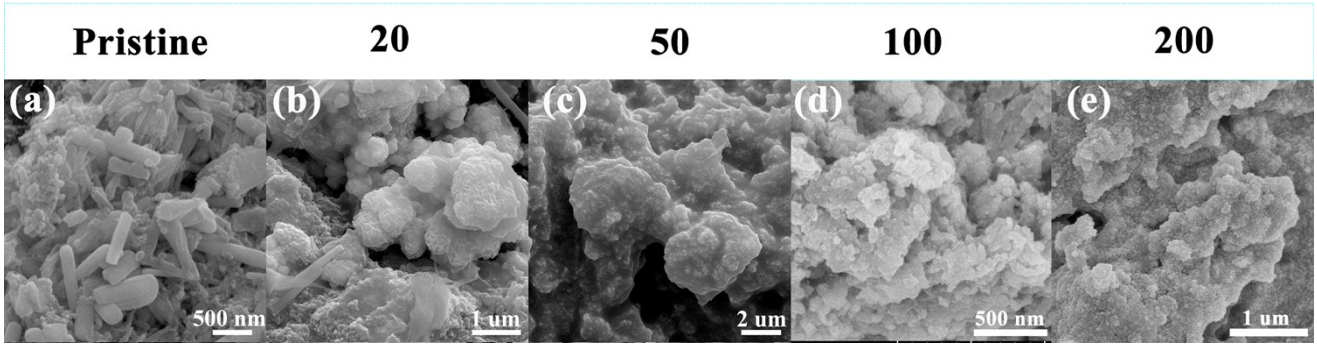

Fig. S5 Ex-situ SEM images of $FeSe_2$@NC electrode for (a) pristine, (b) the 20th cycle, (c) the 50th cycle, (d) the 100th cycle, and (e) the 200th cycle.

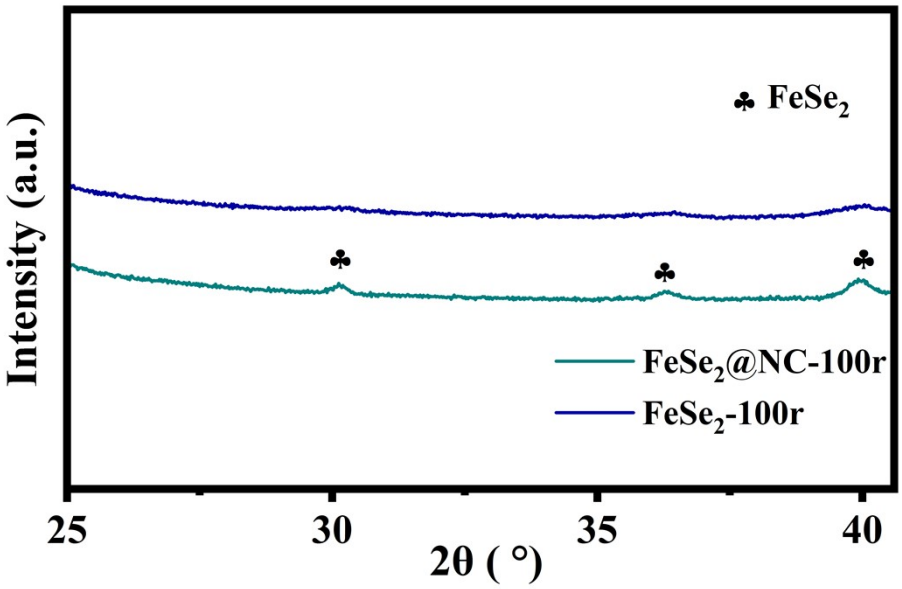

Fig. S6 XRD patterns of $FeSe_2$@NC and $FeSe_2$ after 100 cycles.

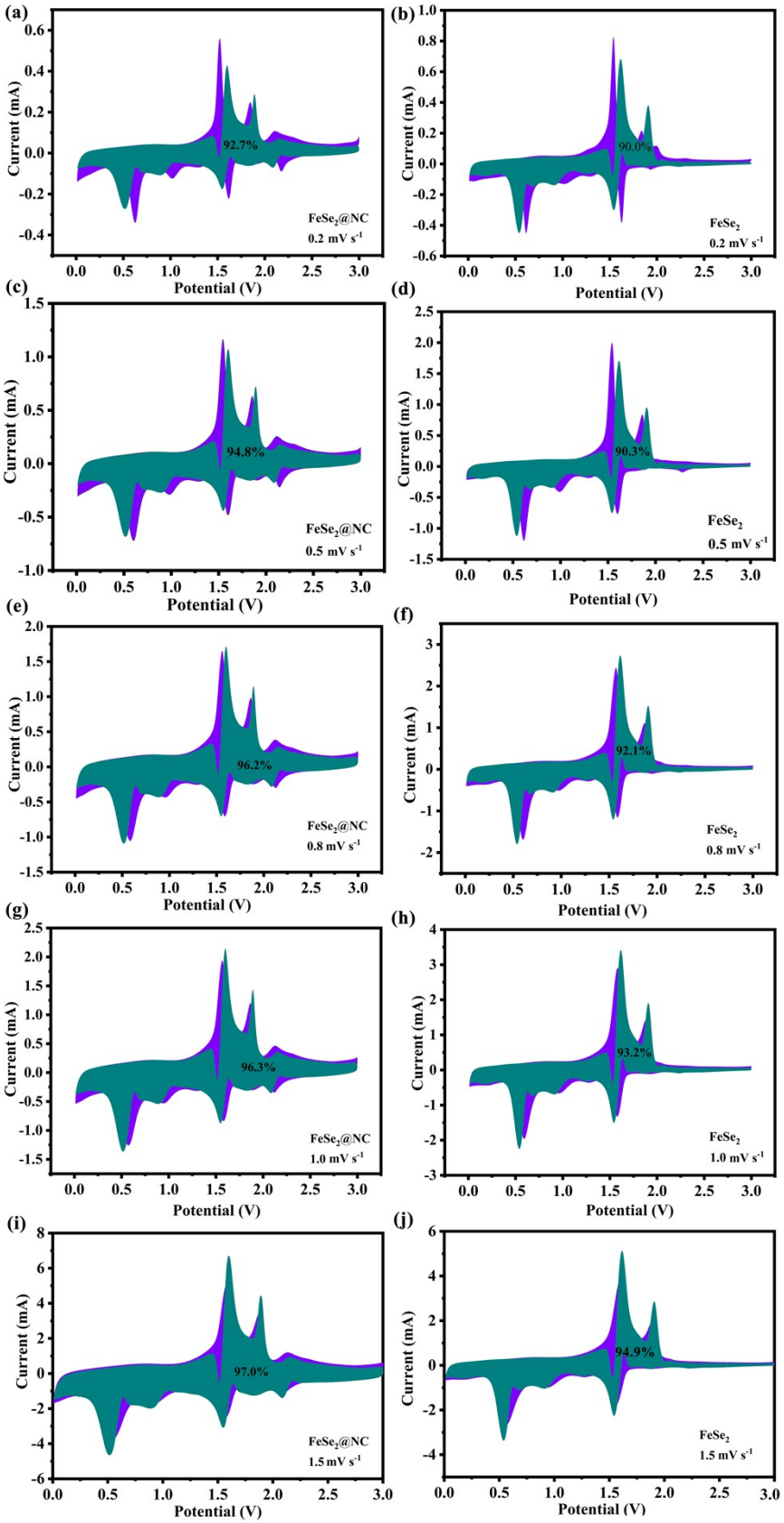

Fig. S7 The pseudocapacitive contribution for $FeSe_2$@NC (a, c, e, g, i) and $FeSe_2$ (b, d, f, h, j) at different scan rates from 0.2 to 1.5 mV s^{-1}.

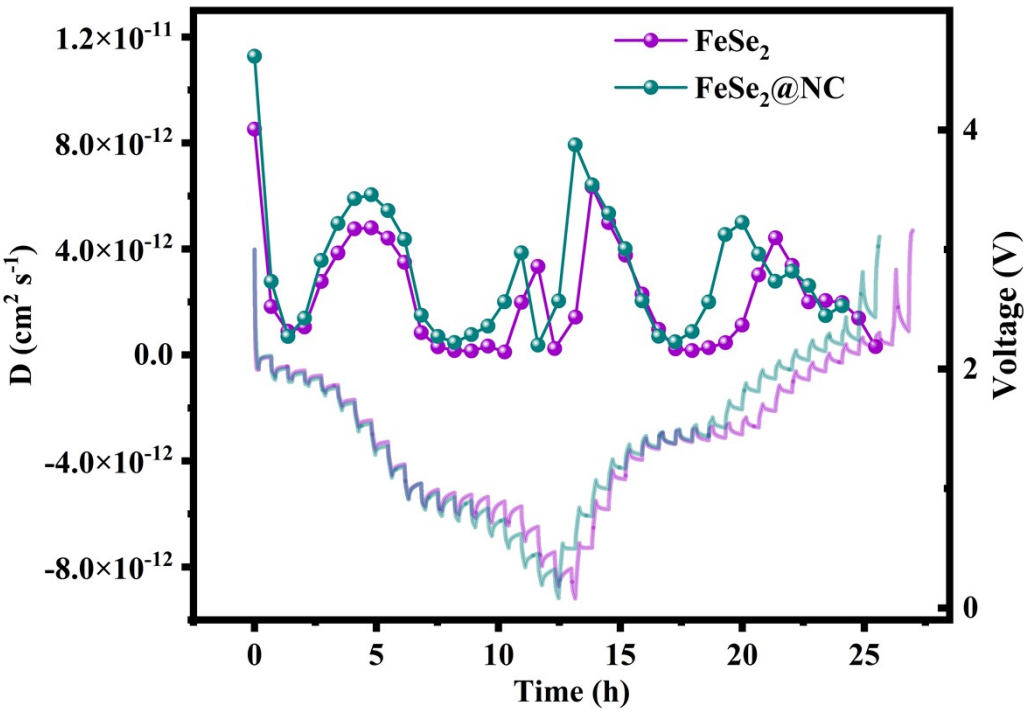

Fig. S8 GITT profiles and Na^+ diffusion coefficient of $FeSe_2$@NC and $FeSe_2$.

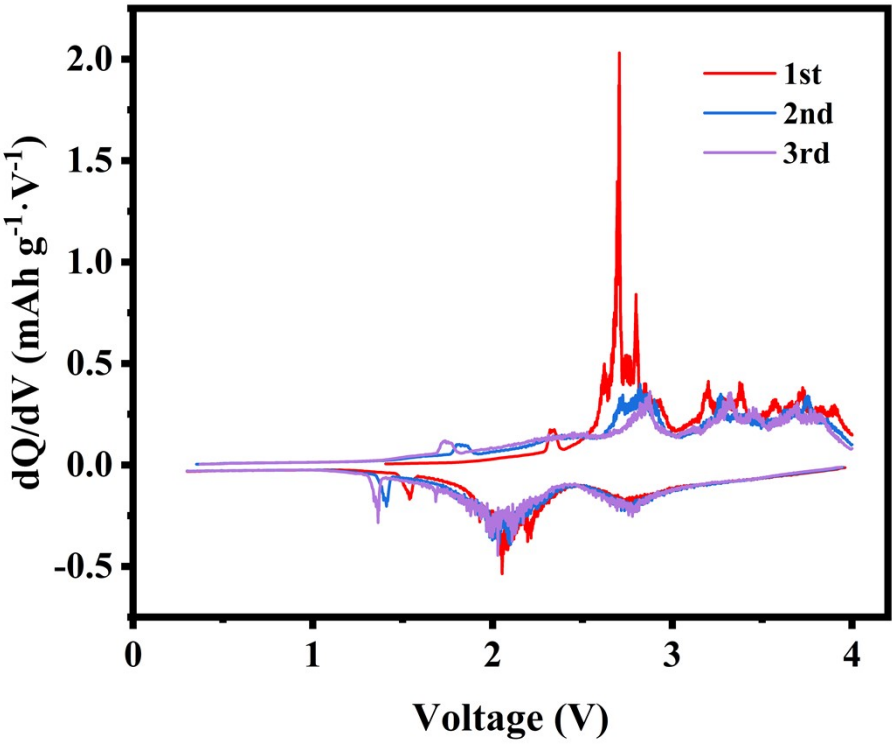

Fig. S9 The differential capacitance curve of $FeSe_2$@NC in the first three cycles.

Table S1. The comparison of electrochemical performance with some reported iron selenides.

Samples	Electrolyte	Initial CE. [%/A g^{-1}]	Rate Capacity [mAh g^{-1}/A g^{-1}]	Cycle Performance [mAh g^{-1}/cycles/A g^{-1}]	Ref
$FeSe_2$@NC	1 M $NaPF_6$ in DEGDME	92.0/0.5	497.4/0.2 379.2/10	443.7/1000/5	This work
Urchin-like Fe_3Se_4 hierarchitectures	1 mol L^{-1} $NaClO_4$ in DEGDME	99.6/0.05	397.2/0.1 200.0/30	390.0/1000/1	1
FeSe-CNFA	1.0 M $NaCF_3SO_3$ in DIGLYME (100 vol %)	68.8/0.1	409.0/0.1 291.0/5	313.0/1000/2	2
$FeSe_2$@C hollow nanocubes	1M $NaClO_4$ in PC with 5% FEC	62.8/0.1	568.0/0.1 245.0/10	212.0/3000/10	3
O-$FeSe_2$NSs	1 M $NaClO_4$ in PC with 5% of FEC	82.9/0.1	387.0/0.1 258.2/3	268.2/700/1	4
Rod $FeSe_2$/N-C	1M $NaCF_3SO_3$ in DEGDME	97.0/0.5	403.0/0.5 207.0/10	308.0/1000/10	5
$FeSe_2$ nanoparticles	1 M $NaPF_6$ in DEGDME	76.0/0.1	520.0/0.5 257.0/10	158.0/2200/2	6
Fe_3Se_4@SiO_2@C	1.0 M $NaCF_3SO_3$ in diglyme	82.1/1	389.0/0.2 302.0/20	323.0/1880/10	7
FeSe@NC	1 M $NaPF_6$ in DEGDME	90.0/0.5	445.0/0.1 364.0/10	318.0/1000/1	8

References

1. J. Zhang, Y. Liu, H. Liu, Y. Song, S. Sun, Q. Li, X. Xing and J. Chen, *Small*, 2020, **16**, 2000504.
2. C. Lv, H. Liu, D. Li, S. Chen, H. Zhang, X. She, X. Guo and D. Yang, *Carbon*, 2019, **143**, 106-115.
3. H. Fan, H. Yu, Y. Zhang, J. Guo, Z. Wang, H. Wang, N. Zhao, Y. Zheng, C. Du, Z. Dai, Q. Yan and J. Xu, *Energy Storage Mater.*, 2018, **10**, 48-55.
4. Z. Wang, B. Zeng, D. Zhou, L. Tai, X. Liu and W. Lau, *Chem. Eng. J.*, 2022, **428**, 132637.
5. P. Ge, H. Hou, S. Li, L. Yang and X. Ji, *Adv. Funct. Mater.*, 2018, **28**, 1801765.
6. F. Zhao, S. Shen, L. Cheng, L. Ma, J. Zhou, H. Ye, N. Han, T. Wu, Y. Li and J. Lu, *Nano Lett.*, 2017, **17**, 4137-4142.
7. W. Zhao, X. Ma, L. Yue, L. Zhang, Y. Luo, Y. Ren, X.-E. Zhao, N. Li, B. Tang, Q. Liu, Y. Liu, S. Gao, A. A. Alshehri and X. Sun, *J. Mater. Chem. A*, 2022, **10**, 4087-4099.
8. S. Wang, T. Cui, L. Shao, S. Yang, L. Yu, J. Guan, X. Shi, J. Cai and Z. Sun, *J. Colloid Interface Sci.*, 2022, **627**, 922-930.